INTERNATIONAL JOURNAL FOR NUMERICAL AND ANALYTICAL METHODS IN GEOMECHANICS
Int. J. Numer. Anal. Meth. Geomech., 2004; **28**:323–337 (DOI: 10.1002/nag.340)

A critical state model for sands dependent on stress and density

Y. P. Yao[1,*,†], D. A. Sun[2] and T. Luo[1]

[1] *Department of Civil Engineering, Beijing University of Aeronautics and Astronautics, Beijing 100083, China*
[2] *Department of Civil Engineering, Nagoya Institute of Technology, Nagoya 466-8555, Japan*

SUMMARY

An elastoplastic model for sands is presented in this paper, which can describe stress–strain behaviour dependent on mean effective stress level and void ratio. The main features of the proposed model are: (a) a new state parameter, which is dependent on the initial void ratio and initial mean stress, is proposed and applied to the yield function in order to predict the plastic deformation for very loose sands; and (b) another new state parameter, which is used to determine the peak strength and describe the critical state behaviour of sands during shearing, is proposed in order to predict simply negative/positive dilatancy and the hardening/softening behaviour of medium or dense sands. In addition, the proposed model can also predict the stress–strain behaviour of sands under three-dimensional stress conditions by using a transformed stress tensor instead of ordinary stress tensor. Copyright © 2004 John Wiley & Sons, Ltd.

KEY WORDS: sands; elastoplastic model; confining stress dependency; density dependency; three dimension

1. INTRODUCTION

The Modified Cam-clay model [1] has been successfully used to describe stress–strain behaviour of normally consolidated clay. To achieve a better agreement between predicted and observed behaviour of sands, a large number of revisions have been proposed since the Modified Cam-clay model was developed. The authors also developed a simple and unified three-dimensional elastoplastic model [2] for both clay and sand by introducing a new hardening parameter H and a new transformed stress tensor $\tilde{\sigma}_{ij}$ to the Modified Cam-clay model.

The mean effective stress level and void ratio are probably the two most significant factors to influence deformation and strength of sands among many factors, such as fabric and inherent anisotropy. If a sample is initially in a very loose state, strain hardening and volume contraction behaviour will be generally observed only, while a medium dense sample may exhibit both volume contraction and dilation as well as strain hardening/softening. On the other hand, the volume dilation of a dense sample may be suppressed totally if the mean effective stress is raised sufficiently.

*Correspondence to: Y. P. Yao, Department of Civil Engineering, Beijing University of Aeronautics and Astronautics, Beijing 100083, China.
† E-mail: ypyao@263.net

Contract/grant sponsor: National Natural Science Foundation of China; contract/grant number: 10272010

Received 13 August 2003
Revised 13 November 2003
Accepted 21 November 2003

In this paper, a unified elastoplastic constitutive model for sands, which can account for the mean effective stress level and void ratio dependencies, is proposed. The main features of the proposed model are: (1) a new state parameter χ_1, which is dependent on the initial void ratio and initial mean stress, is proposed and applied to the yield function in order to predict the plastic deformation for very loose sands; and (2) another new state parameter χ_2, which is used to determine the peak strength M_f and describes the critical state behaviour of sands during shearing, is proposed in order to predict simply negative/positive dilatancy and the hardening/softening behaviour of medium or dense sands. In addition, the proposed model can also predict the stress–strain behaviour of sands under three-dimensional stress conditions by using a transformed stress tensor [3] $\tilde{\sigma}_{ij}$ based on the spatially mobilized plane (SMP) criterion [4, 5] instead of ordinary stress tensor σ_{ij}. Throughout this paper, the term 'stress' is to be interpreted as 'effective stress'.

2. DEFINITION OF STATE PARAMETERS χ_1 AND χ_2

2.1. Dilatancy and peak strength of sands dependent on stress level and void ratio

Several basic lines are shown in v (specific volume) – ln p (mean stress) space in Figure 1. It is experimentally confirmed that there exists a critical state line (CSL) where every sand sample reaches infinite shear strain irrespective of initial void ratio in the same way as normally consolidated clay [6]. The slope of CSL is assumed λ. The reference consolidation line in Figure 1, which is similar to the normal consolidation line for normally consolidated clay, is called RCL. RCL is assumed to be parallel with CSL as shown in Figure 1. So, the slope of RCL is also λ. RCL is not a locus of points of maximum possible void ratio. The distance between RCL and CSL is assumed to be $(\lambda - \kappa)\ln 2$ based on the Modified Cam-clay model in which the distance between normal consolidation line and critical state line is $(\lambda - \kappa)\ln 2$ at the same mean stress. When a sample is sheared from an initial state on RCL, it shows only volume contraction

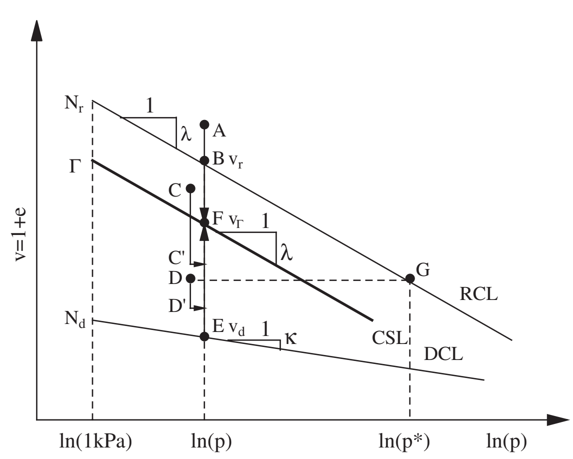

Figure 1. Description of dilatancy of sand with different initial densities in v–ln p plane.

(negative dilatancy). When a sample is sheared from an initial state looser than RCL, it also shows only volume contraction, but a negative dilatancy larger than that from the initial state on RCL. On the other hand, sand denser than RCL shows both negative and positive dilatancy. The isotropic consolidation line for the densest possible state of sand is the lowest boundary line and its slope is equal to the slope of the unloading or reloading line, which is called DCL in Figure 1. The slope of DCL is κ.

In Figure 1, v_r, v_Γ and v_d are three values of specific volume for a given mean stress p on RCL, CSL and DCL respectively; N_r, Γ and N_d are the values of specific volume for unit mean stress on RCL, CSL and DCL respectively, which are three basic void ratio parameters of sand. From Figure 1, the following three equations can be obtained:

$$v_r = N_r - \lambda \ln p \tag{1}$$

$$v_\Gamma = \Gamma - \lambda \ln p \tag{2}$$

$$v_d = N_d - \kappa \ln p \tag{3}$$

Figure 1 also shows different dilatancy behaviour of sand with different initial void ratios in v–ln p space. The dilatancy of sand for a given initial void ratio (e.g. points A, B, C, D and E in Figure 1) is analysed as follows:

(1) Point B: When a sample is sheared from an initial state at point B on RCL, sand behaves only volume contraction (negative dilatancy) and finally reaches the critical state (point F on CSL). In this condition that the initial state is on RCL, the dilatancy of sand is the same as that of the normally consolidated clay. Hence, the Modified Cam-clay model can be used to predict the stress–strain relationship of sand in this state.
(2) Point A: When a sample is sheared from an initial state at point A looser than RCL, it shows only also volume contraction (negative dilatancy) and finally reaches the critical state (point F on CSL). But sand in this state exhibits a volume contraction larger than that at the initial state of point B. The Modified Cam-clay model cannot be used to predict directly the stress–strain relationship of sand in this state.
(3) Points C and D: The sample denser than RCL (e.g. for initial state at points C and D) shows positive dilatancy after volume contraction and then reaches the same critical state (C → C′ → F and D → D′ → F) as the loose sand. It should be noted that although points C and B are all higher than the point F on CSL under the same mean stress in v–ln p space, the dilatancy of sand from points C and B is different and sand from point C shows positive dilatancy after negative dilatancy. Points C′ and D′ are characteristic points [7, 8] in Figure 1.
(4) Point E: When the densest possible sample is sheared from an initial state at point E on DCL, it shows almost positive dilatancy and finally reaches critical state (E → F).

Sand in different initial void ratios reaches different peak shear strengths. Figure 2 shows that sand denser than RCL reaches shear strength greater than M, which is a shear strength for sand on RCL, and the denser the sand, the greater its shear strength. However, sand looser than RCL reaches the same shear strength as sand on RCL. That is $(\eta_{\max})_E > (\eta_{\max})_D > (\eta_{\max})_C > (\eta_{\max})_B = (\eta_{\max})_A = M$ with $\eta_{\max}$ as a maximum stress ratio.

Comparing points D and G whose initial void ratios are the same, as shown in Figure 1, we can find a value of p^* at which only volume contraction occurs during shearing. So soon as the

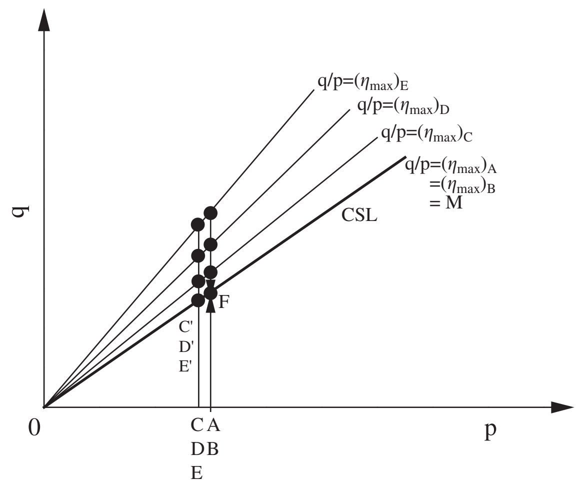

Figure 2. Description of peak strength of sand with different initial densities in p–q plane.

mean stress is raised to p^* (point G from point D in Figure 1) the volume dilation of sand may be suppressed totally.

From the above discussions, we can know how both the mean stress and initial void ratio affect the dilatancy and strength of sands.

2.2. State parameters χ_1, χ_2 and their application

Considerable research efforts have been directed at investigating the effects of the mean stress level and void ratio on the dilatancy and peak strength of sands. In order to describe these effects, several typical state parameters [8–15] have been proposed, respectively.

In order to take the mean stress level and void ratio dependencies into consideration in modelling sand behaviour, two new state parameters are proposed here. A new state parameter χ_1 is proposed to predict the plastic deformation for the initial state looser than RCL and another new state parameter χ_2 is proposed to predict the peak strength M_f of sand for the initial state denser than RCL.

2.2.1. State parameter χ_1 and yield function. For a given sand whose initial void state is on RCL in Figure 3, we can calculate its plastic volumetric strain during shearing by the Modified Cam-clay model, in which the yield function can be written as follows:

$$f = \ln\frac{p}{p_0} + \ln(1+\eta^2/M^2) - \int \frac{\mathrm{d}\varepsilon_v^{\mathrm{p}}}{c_p} = 0 \tag{4}$$

where p_0 is the initial mean stress, $\eta(= q/p)$ the stress ratio, M the value of η at the critical state, $\mathrm{d}\varepsilon_v^{\mathrm{p}}(= \mathrm{d}\varepsilon_{ii}^{\mathrm{p}})$ the plastic volumetric strain increment and

$$c_p = \frac{\lambda-\kappa}{1+e_0} \tag{5}$$

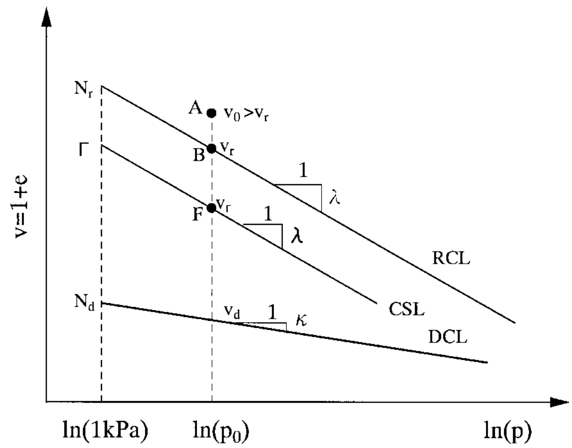

Figure 3. Sand looser than RCL expressed by point A.

where λ is the slope of normal consolidation line or critical state line, κ the swelling index and e_0 the initial void ratio at $p = p_0$. We can calculate the increment of specific volume between point B and point F in Figure 3, based on Equation (4) as follows:

$$v_r - v_\Gamma = (\lambda - \kappa)\ln(1 + \eta^2/M^2)|_{\eta=M} = (\lambda - \kappa)\ln 2 \tag{6}$$

From Equations (1), (2) and (6), we can also obtain $N_r = \Gamma + (\lambda - \kappa)\ln 2$. However, when sand looser than RCL is sheared, its increment of specific volume is larger than the value of $(v_r - v_\Gamma)$ (e.g. from point A to point F in Figure 3), i.e. $(v_0 - v_\Gamma) > (v_r - v_\Gamma)$. Here a new state parameter χ_1 is proposed to calculate the value of $(v_0 - v_\Gamma)$. Let

$$v_0 - v_\Gamma = (\lambda - \kappa)\ln\left(1 + \frac{\eta^2/M^2}{1 - \chi_1\eta^2/M^2}\right)\Bigg|_{\eta=M} = (\lambda - \kappa)\ln\left(1 + \frac{1}{1 - \chi_1}\right) \quad (0 \leqslant \chi_1 \leqslant 1) \tag{7}$$

where $(v_0 - v_\Gamma) = (v_r - v_\Gamma)$ when $\chi_1 = 0$, $(v_0 - v_\Gamma) > (v_r - v_\Gamma)$ when $\chi_1 > 0$ and $(v_0 - v_\Gamma) \to \infty$ when $\chi_1 = 1$. If we know the initial value of specific volume v_0, then the state parameter χ_1 can be solved from Equation (7) as follows:

$$\chi_1 = \frac{\exp\left(\dfrac{v_0 - v_\Gamma}{\lambda - \kappa}\right) - 2}{\exp\left(\dfrac{v_0 - v_\Gamma}{\lambda - \kappa}\right) - 1} \tag{8}$$

Substituting Equation (2) into Equation (8) gives

$$\chi_1 = \frac{\exp\left(\dfrac{v_0 - \Gamma + \lambda\ln p_0}{\lambda - \kappa}\right) - 2}{\exp\left(\dfrac{v_0 - \Gamma + \lambda\ln p_0}{\lambda - \kappa}\right) - 1} \tag{9}$$

From Equation (9), it can be seen that the parameter χ_1 can be calculated from the initial value of specific volume v_0 and initial mean stress p_0. So, χ_1 is not a material parameter but an initial state variable. By comparing Equation (6) with (7), the yield function, with which the deformation behaviour of sand looser than RCL can be accounted for, is written as follows:

$$f = \ln\frac{p}{p_0} + \ln\left(1 + \frac{\eta^2/M^2}{1 - \chi_1\eta^2/M^2}\right) - \int\frac{d\varepsilon_v^p}{c_p} = 0 \tag{10}$$

When $\chi_1 = 0$, Equation (10) is the same as Equation (4), which is the yield function of the Modified Cam-clay model. Here, it should be noted that $\chi_1 = 0$ when sand is denser than RCL. Figure 4 shows the yield loci drawn by Equation (10) when the state parameter $\chi_1 = 0.00$, 0.25, 0.50, 0.75 and 1.00 respectively.

2.2.2. State parameter χ_2, peak strength M_f and hardening/softening parameter H. Another new state parameter χ_2 is introduced to describe the peak strength and dilatancy of sand denser than RCL, which is defined as

$$\chi_2 = \frac{v_\eta - v}{v_r - v_d} \tag{11}$$

where v_η is the value of specific volume, equivalent to the value in the normal consolidation condition for a given mean stress p and stress ratio η as shown in Figure 5, $(v_\eta - v)$ is the difference in specific volume between the state of stress ratio η and the current void state for a given mean stress p in Figure 5. $(v_r - v_d)$ is the difference in specific volume between RCL and DCL for the mean stress p (Figure 5). $(v_r - v_d)$ and $(v_\eta - v)$ can also be written as follows:

$$(v_r - v_d) = (N_r - N_d) - (\lambda - \kappa)\ln p \tag{12}$$

$$\begin{aligned}(v_\eta - v) &= (v_r - v) - (v_r - v_\eta)\\ &= (v_r - v^p - v^e) - (v_r - v_\eta^p - v^e)\\ &= (v_r - v^p) - (v_r - v_\eta^p)\end{aligned} \tag{13}$$

where

$$(v_r - v^p) = N_r - \lambda\ln p_0 - v_0(1 - \varepsilon_v^p) \tag{14}$$

$$(v_r - v_\eta^p) = (\lambda - \kappa)\ln\left\{\frac{p}{p_0}\left(1 + \frac{\eta^2}{M^2}\right)\right\} \tag{15}$$

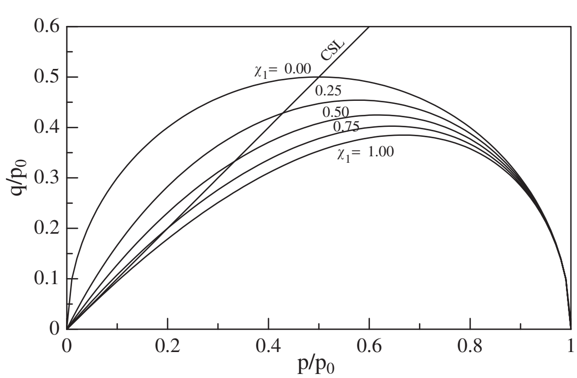

Figure 4. Yield loci of sand for different values of state parameter χ_1.

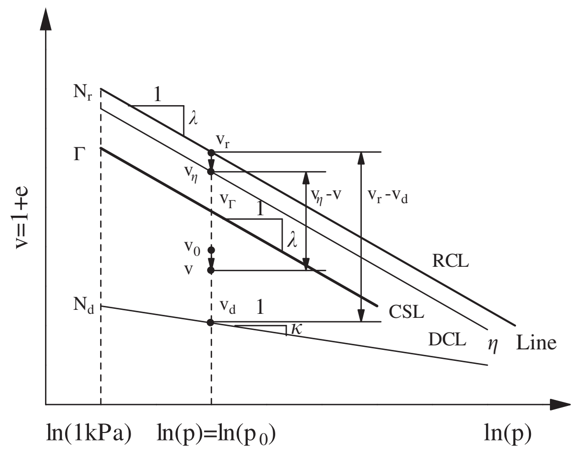

Figure 5. Definition of state parameter χ_2.

Substituting Equations (12)–(15) into Equation (11) gives

$$\chi_2 = \frac{\{N_r - \lambda \ln p_0 - v_0(1-\varepsilon_v^{\mathrm{p}})\} - (\lambda - \kappa)\ln\left\{\dfrac{p}{p_0}\left(1+\dfrac{\eta^2}{M^2}\right)\right\}}{(N_r - N_d) - (\lambda-\kappa)\ln p} \quad (0 \leqslant \chi_2 \leqslant 1) \tag{16}$$

It can be seen from Equation (16) that the state parameter χ_2 correlates both the initial state values (v_0, p_0 and $\eta_0 = 0$) and the current state values ($v(\varepsilon_v^{\mathrm{p}})$, p and η). So, this parameter can rationally account for the dependency of sand behaviour on the mean stress level and void ratio during shearing.

The peak strength M_f of sand denser than RCL is assumed to be a function of state parameter χ_2 as follows:

$$M_f = (M_{f\max} - M)\sqrt{\chi_2} + M \tag{17}$$

where M is the stress ratio at the characteristic or critical state, $M_{f\max}$ the maximum possible peak strength which is a soil parameter and can be determined by test results of sand. $M_{f\max}$ can be found from a triaxial compression test on a maximum density sample at any confining pressure. From Equation (17), when the initial state of sand is on RCL ($\chi_2 \equiv 0$), $M_f = M$, while $M_f = M_{f\max}$ when the initial state of sand is on DCL ($\chi_2 = 1$).

Figure 6 shows the comparison between experimental results and calculated results (Equation (17)) about peak strength M_f and state parameter χ_2 for Toyoura sand. The calculations were conducted using $M_{f\max} = 1.93$, $M = 1.05$, which are listed in Table I. Also from Figure 6, it can be seen that Equation (17) can predict peak strength rationally.

The yield function like Equation (10) cannot describe the dilatancy of sand denser than RCL when the plastic volumetric strain is used as the hardening parameter. Therefore, it is necessary to introduce a new hardening/softening parameter H to Equation (10) so as to transform it into a more general yield function:

$$f = \ln\frac{p}{p_0} + \ln\left(1 + \frac{\eta^2/M^2}{1-\chi_1\eta^2/M^2}\right) - H = 0 \tag{18}$$

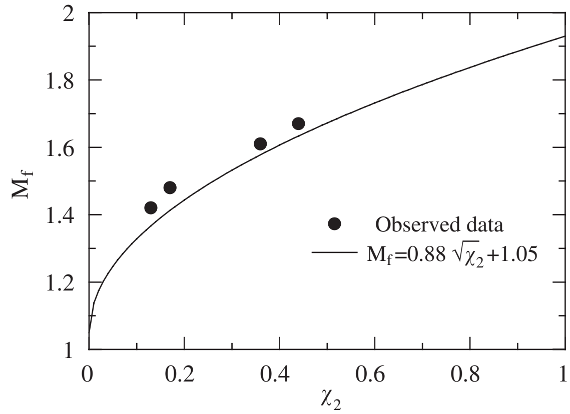

Figure 6. Comparison between predicted and observed shear strength for Toyoura sand (experimental data after Nakai *et al.* [13]).

Table I. Soil parameters used in model predictions.

λ	κ	Γ	N_d	M	$M_{f\max}$	v
0.09	0.02	2.40	1.69	1.05	1.93	0.00

Based on experimental results of triaxial tests on clay and sand, we have proposed a hardening parameter for a hardening elastoplastic model for soils exhibiting negative and positive dilatancy [2]. Here, the hardening parameter is extended to a new hardening/softening parameter as follows:

$$H = \int \mathrm{d}H = \int \frac{1}{\bar{c}_p} \frac{M^4}{M_f^4} \frac{M_f^4 - {\eta^*}^4}{M^4 - {\eta^*}^4} \mathrm{d}\varepsilon_v^{\mathrm{p}} \tag{19}$$

$$\eta^* = \begin{cases} \eta & \mathrm{d}\eta \geqslant 0 \\ \eta_{\max} & \mathrm{d}\eta < 0 \end{cases} \tag{20}$$

where $\eta_{\max}$ is the maximum stress ratio during shearing, $\bar{c}_p$ is plastic index for denser sand and is assumed as

$$\bar{c}_p = \frac{\bar{\lambda} - \kappa}{1 + e_0} = c_p \frac{M^4}{M_f^4} = \frac{\lambda - \kappa}{1 + e_0} \frac{M^4}{M_f^4} \tag{21}$$

where $\bar{\lambda}$ is the slope of the consolidation lines for sand denser than RCL. The swelling slope κ is assumed to be constant for all cases. However, the slope $\bar{\lambda}$ of the consolidation lines for specimens consolidated from different initiate states (for example, C or D in Figure 1) are different, which are seen from the calculation of $\bar{c}_P$ in Equation (21). So, $\kappa \leqslant \bar{\lambda} \leqslant \lambda$. From Equation (21), it can be seen that $\bar{c}_p = c_p$, i.e. $\bar{\lambda} = \lambda$ when $M_f = M$ for normally consolidated clay, and $\bar{c}_p$ reaches the least value when $M_f = M_{f\max}$.

Substituting Equation (21) into Equation (19) gives

$$H = \int \mathrm{d}H = \int \frac{1}{c_p} \frac{M_f^4 - \eta^{*^4}}{M^4 - \eta^{*^4}} \mathrm{d}\varepsilon_v^{\mathrm{p}} \tag{22}$$

From Equation (19), we can get

$$\mathrm{d}\varepsilon_v^{\mathrm{p}} = \bar{c}_p \frac{M_f^4}{M^4} \frac{M^4 - \eta^{*^4}}{M_f^4 - \eta^{*^4}} \mathrm{d}H \tag{23}$$

It can be known from the stress-dilatancy equation that the stress ratio η^* is a function of the ratio of plastic volumetric strain to plastic shear strain. Hence, the hardening/softening parameter H can be considered as a combination of plastic volumetric strain and plastic shear strain from Equation (19). Since H is a hardening/softening parameter, $\mathrm{d}H$ is larger than zero before peak strength and is less than zero after peak strength. Taking these into account, the following features can be deduced from Equation (23):

(1) When $\eta = 0$ or $M_f = M$, $\mathrm{d}H = \mathrm{d}\varepsilon_v^{\mathrm{p}}/\bar{c}_p$, i.e. the hardening/softening parameter H becomes the plastic volumetric strain $\varepsilon_v^{\mathrm{p}}/\bar{c}_p$, which is the same as the hardening parameter in the Cam-clay model.
(2) In the case of $\mathrm{d}H > 0$, when $0 < \eta < M$, $\mathrm{d}\varepsilon_v^{\mathrm{p}} > 0$; when $\eta = M$, $\mathrm{d}\varepsilon_v^{\mathrm{p}} = 0$; and when $M < \eta < \eta_{\max}$, $\mathrm{d}\varepsilon_v^{\mathrm{p}} < 0$. That is, negative and positive dilatancy of sand is described in the hardening zone.
(3) In the case of $\mathrm{d}H < 0$, when $M < \eta < \eta_{\max}, \eta^* = \eta_{\max}$ and $M < M_f < \eta_{\max}$, $\mathrm{d}\varepsilon_v^{\mathrm{p}} < 0$, i.e. positive dilatancy of sand is described in the softening zone.
(4) In the case of $\mathrm{d}H = 0$, when $\eta = M_f = \eta_{\max}$, $\mathrm{d}\varepsilon_v^{\mathrm{p}} < 0$, i.e. peak strength of sand is described, and when $\eta = M$, $M_f = M$, $\mathrm{d}\varepsilon_v^{\mathrm{p}} = 0$, i.e. critical state condition is described.

The nature of the hardening process in the proposed model is explained as follows.

In the Modified Cam-clay model, since the hardening law in isotropic stress for normally consolidated clays is assumed as $\int (1+e_0)/(\lambda - \kappa)\, \mathrm{d}\varepsilon_v^{\mathrm{p}} = \ln p/p_0$, the general hardening law during shearing can be written as

$$\int \frac{1+e_0}{\lambda - \kappa} \mathrm{d}\varepsilon_v^{\mathrm{p}} = \ln \frac{p_x}{p_0} \tag{24}$$

where p_x is a value in p axes on the yield surface corresponding to current stress state, p_0 the initial mean stress and $\mathrm{d}\varepsilon_v^{\mathrm{p}}$ the plastic volumetric strain increment during shearing.

Similarly, the nature of the hardening process described by the hardening/softening parameter H for sands is that a hardening law $\int (1+e_0)/(\bar{\lambda} - \kappa)\, \mathrm{d}\varepsilon_v^{\mathrm{p}} = \ln p/p_0$ in isotropic stress is extended to a general hardening law:

$$\int \frac{1+e_0}{\bar{\lambda} - \kappa} \frac{M^4 (M_f^4 - \eta^{*^4})}{M_f^4 (M^4 - \eta^{*^4})} \mathrm{d}\varepsilon_v^{\mathrm{p}} = \ln \frac{p_x}{p_0} \tag{25}$$

By comparing Equation (24) with (25), we can see that it is a coefficient concerning stress ratio η^* in front of $\mathrm{d}\varepsilon_v^{\mathrm{p}}$ in Equation (25) that adjusts the positive or negative value of $\mathrm{d}\varepsilon_v^{\mathrm{p}}$. That is, positive and negative dilatancy of sands can be described in the hardening zone.

Since the peak strength M_f is not a constant but a function of state parameter χ_2 and finally reaches the critical state stress ratio M when $\chi_2 = 0$ according to Equation (17), the softening behaviour and positive dilatancy of sands after the peak strength can also be modelled according to Equation (23) and the following constitutive equation.

The direction of the plastic strain increment is always directed outward from the current yield surface and plastic potential surface. The yield surface may increase in size with positive dH in the hardening zone (positive volumetric strain increment for $0<\eta<M$; negative volumetric strain increment for $M<\eta<M_f$), and may decrease in size with negative dH in the softening zone (negative volumetric strain increment).

3. MATHEMATICAL DESCRIPTION OF STRESS–STRAIN BEHAVIOUR OF SANDS

3.1.3. 3-D method using transformed stress tensor on SMP criterion

A transformed stress tensor $\tilde{\sigma}_{ij}$, by which the SMP criterion [4, 5] could be drawn as a circle in the transformed π-plane, has been proposed by authors [3]. In the condition that the principal directions of $\tilde{\sigma}_{ij}$ and σ_{ij} are the same, the transformed stress tensor $\tilde{\sigma}_{ij}$ can be written by

$$\tilde{\sigma}_{ij} = \tilde{p}\delta_{ij} + \tilde{s}_{ij} = p\delta_{ij} + \frac{\ell_0}{\sqrt{s_{kl}s_{kl}}} s_{ij} \tag{26}$$

where δ_{ij} is Kronecker's delta, s_{ij} the deviatoric stress tensor, $\tilde{p}$ the mean transformed stress and $\tilde{s}_{ij}$ the deviatoric transformed stress tensor:

$$\tilde{p} = \tfrac{1}{3}\tilde{\sigma}_{ii} \tag{27}$$

$$\tilde{s}_{ij} = \tilde{\sigma}_{ij} - \tilde{p}\delta_{ij} \tag{28}$$

ℓ_0 is the radius of the SMP curve along triaxial compression stress path, which is written by [3]

$$\ell_0 = \sqrt{\frac{2}{3}} \frac{2I_1}{3\sqrt{(I_1 I_2 - I_3)/(I_1 I_2 - 9I_3)} - 1} \tag{29}$$

where I_1, I_2 and I_3 are, respectively, the first, second and third stress invariants.

3.2. Modelling stress–strain relation of sands

In the proposed elastoplastic model, Equation (18) is used as the yield function and the plastic potential function is assumed to be the same as that of the Modified Cam-clay model (i.e. $g = \ln p/p_0 + \ln(1 + \eta^2/M^2)$), but the transformed stress tensor $\tilde{\sigma}_{ij}$ based on the SMP criterion is adopted to model the stress–strain behaviour of sands in three-dimensional stresses.

The total strain increment is given by the summation of the elastic component and the plastic component as usual

$$\mathrm{d}\varepsilon_{ij} = \mathrm{d}\varepsilon_{ij}^{\mathrm{e}} + \mathrm{d}\varepsilon_{ij}^{\mathrm{p}} \tag{30}$$

Here, the elastic component $\mathrm{d}\varepsilon_{ij}^{\mathrm{e}}$ is given by Hooke's law, i.e.

$$\mathrm{d}\varepsilon_{ij}^{\mathrm{e}} = \frac{1+v}{E}\mathrm{d}\sigma_{ij} - \frac{v}{E}\mathrm{d}\sigma_{mm}\delta_{ij} \tag{31}$$

where v is Poisson's ratio and elastic modulus E is expressed as

$$E = \frac{3(1-2v)(1+e_0)}{\kappa} p \tag{32}$$

And, the plastic component $d\varepsilon_{ij}^{p}$ is given by assuming the flow rule to obey not in σ_{ij}-space but in the $\tilde{\sigma}_{ij}$-space

$$d\varepsilon_{ij}^{p} = \Lambda \frac{\partial g}{\partial \tilde{\sigma}_{ij}} \tag{33}$$

Because the transformed stress takes place of the ordinary stress in the model, the basic equations of the proposed elastoplastic model are given in details respectively as follows:

The yield function f is written as

$$f = \ln \frac{\tilde{p}}{\tilde{p}_0} + \ln\left(1 + \frac{\tilde{\eta}^2/M^2}{1 - \chi_1 \tilde{\eta}^2/M^2}\right) - \tilde{H} = 0 \tag{34}$$

The plastic potential function g is written as

$$g = \ln \frac{\tilde{p}}{\tilde{p}_0} + \ln\left(1 + \frac{\tilde{\eta}^2}{M^2}\right) = 0 \tag{35}$$

The hardening/softening parameter $\tilde{H}$ for 3D stress condition is extended from Equation (22) to

$$\tilde{H} = \int d\tilde{H} = \int \frac{1}{c_p} \frac{M_f^4 - \tilde{\eta}^{*4}}{M^4 - \tilde{\eta}^{*4}} d\varepsilon_v^{p} \tag{36}$$

$$\tilde{\eta}^{*} = \begin{cases} \tilde{\eta} & d\tilde{\eta} \geqslant 0 \\ \tilde{\eta}_{\max} & d\tilde{\eta} < 0 \end{cases} \tag{37}$$

The proportionality constant Λ and the stress gradient $\partial g/\partial \tilde{\sigma}_{ij}$ are written respectively as follows:

$$\Lambda = \bar{c}_p \frac{M^4 - \tilde{\eta}^{*4}}{M_f^4 - \tilde{\eta}^{*4}} \frac{(M^2 + \tilde{\eta}^2)}{(M^2 - \tilde{\eta}^2)(M^2 - \chi_1 \tilde{\eta}^2)} \cdot \frac{\{M^4 - (1 + 2\chi_1)M^2\tilde{\eta}^2 - \chi_1(1 - \chi_1)\tilde{\eta}^4\}\, d\tilde{p} + 2M^2 \tilde{\eta}\, d\tilde{q}}{M^2 + (1 - \chi_1)\tilde{\eta}^2} \tag{38}$$

$$\frac{\partial g}{\partial \tilde{\sigma}_{ij}} = \frac{1}{M^2 \tilde{p}^2 + \tilde{q}^2} \left\{ \frac{M^2 \tilde{p}^2 - \tilde{q}^2}{3\tilde{p}} \delta_{ij} + 3(\tilde{\sigma}_{ij} - \tilde{p}\delta_{ij}) \right\} \tag{39}$$

In the above equations, $\tilde{q}$, $\tilde{\eta}$ and M($\tilde{\eta}$ at critical state) are written respectively as follows:

$$\tilde{q} = \sqrt{\tfrac{3}{2}(\tilde{\sigma}_{ij} - \tilde{p}\delta_{ij})(\tilde{\sigma}_{ij} - \tilde{p}\delta_{ij})} \tag{40}$$

$$\tilde{\eta} = \tilde{q}/\tilde{p} \tag{41}$$

$$M = \frac{3 \sin \phi}{6 - \sin \phi} \tag{42}$$

where ϕ is the friction angle at the characteristic or critical state.

The model predictions for different values of initial void ratio and initial mean stresses are presented in the following section.

4. PREDICTIONS OF MODEL

The effects of mean stress and initial void ratio on sand behaviour are investigated for Toyoura sand in drained and undrained triaxial conditions using the proposed elastoplastic model. The model has 7 soil parameters ($\lambda, \kappa, \Gamma, N_d, M, M_{f\max}$ and ν), which can be all determined from the results of conventional tests on sand. Table I lists out all the soil parameters used in the following model predictions. These values were borrowed from the literatures for Toyoura sand [6, 13, 16].

4.1. *Effect of state parameter* χ_1

Two values of initial void ratio, i.e. $e_0 = 0.89$ and 0.97, were used in the analysis of triaxial conditions at a mean stress of $p = 490$ kPa. Figure 7 shows the influence of void ratio looser than RCL on the response of sand in triaxial compression and extension, respectively. It can be seen from Figure 7 that the sand ($e_0 = 0.97$) looser than RCL tends to the same strength as sand on RCL ($e_0 = 0.89$) but looser sand ($e_0 = 0.97$) shows a larger volume contraction.

4.2. *Effect of state parameter* χ_2

The strength and dilatancy of sand denser than RCL are predicted at different initial void ratios and different mean stresses as follows.

4.2.1. Effect of initial void ratio. Three values of initial void ratio, i.e. $e_0 = 0.68$, 0.77 and 0.85, were used in the analysis of triaxial conditions at a mean stress of $p = 196$ kPa. Figure 8 clearly shows the influence of the initial void ratio on the stress–strain response of sand in triaxial compression and extension conditions, respectively. In Figure 8, the stress–strain curves present the peak strength increases with initial void ratio decreasing. The corresponding volume change is also given in Figure 8, which shows that the volume change is different for different initial states.

4.2.2. Effect of mean stress level. The sand with the initial void ratio fixed at $e_0 = 0.77$ and mean stresses of $p = 196$, 490 and 784 kPa was used to discuss the dilatancy dependent on mean

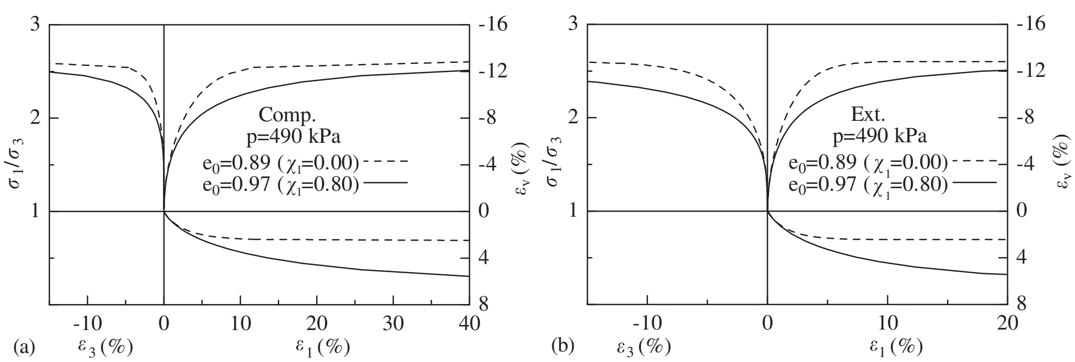

Figure 7. Effect of initial density looser than RCL (state parameter χ_1) on stress–strain behaviour of sand in drained triaxial tests.

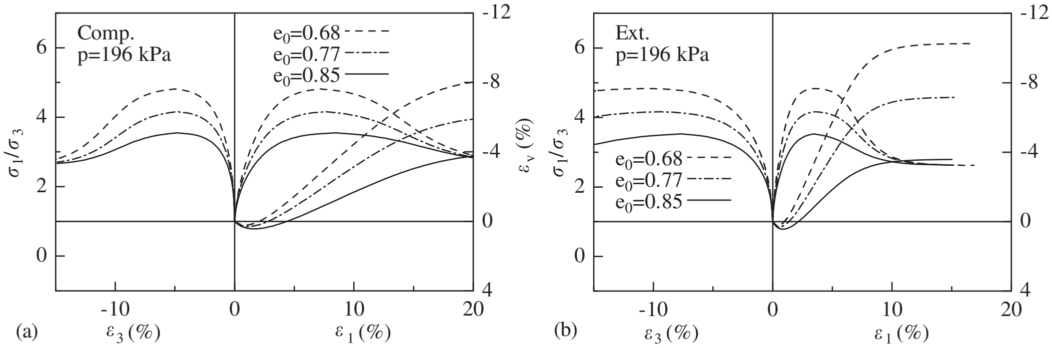

Figure 8. Effect of initial density denser than RCL on stress–strain behaviour of sand in drained triaxial tests.

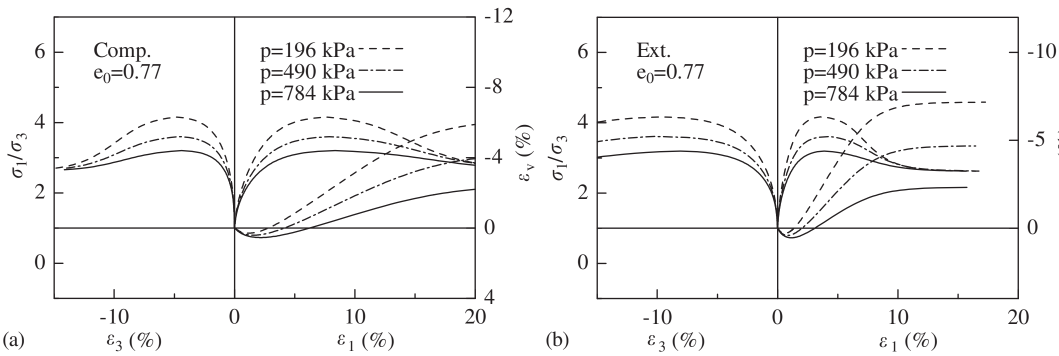

Figure 9. Effect of mean stress on stress–strain behaviour of sand in drained triaxial tests.

stress level. Figure 9 shows the predicted results in that the post peak softening behaviour gradually decreases with increasing mean stress. In fact, at higher mean stress for the same initial void ratio, the volume dilation of sand may be suppressed completely.

4.3. *Prediction in undrained triaxial tests*

Five values of initial void ratio, i.e. $e_0 = 0.762$, 0.861, 0.883, 0.930 and 0.970, were used in the analysis of undrained triaxial tests at an initial mean stress of $p_0 = 490$ kPa in Figure 10. Four values of initial mean stress, i.e. $p_0 = 98$, 980, 1960 and 2940 kPa, were used in the analysis of undrained triaxial tests at an initial void ratio of $e_0 = 0.833$ in Figure 11. The predicted stress–strain behaviour in Figures 10 and 11 clearly shows how the initial void ratio and initial mean stress influence the stress–strain response of the sand in undrained triaxial compression tests. These trends are the same as the experimental results [6, 17, 18].

4.4. *Prediction and experiment in drained triaxial tests*

Figure 12 shows the observed results [13] (dots) and predicted curves of triaxial compression and extension tests respectively under constant mean stress ($p = 196$ kPa) on Toyoura sand ($e_0 = 0.68$ and 0.85). Although the soil parameters used are completely the same, the proposed

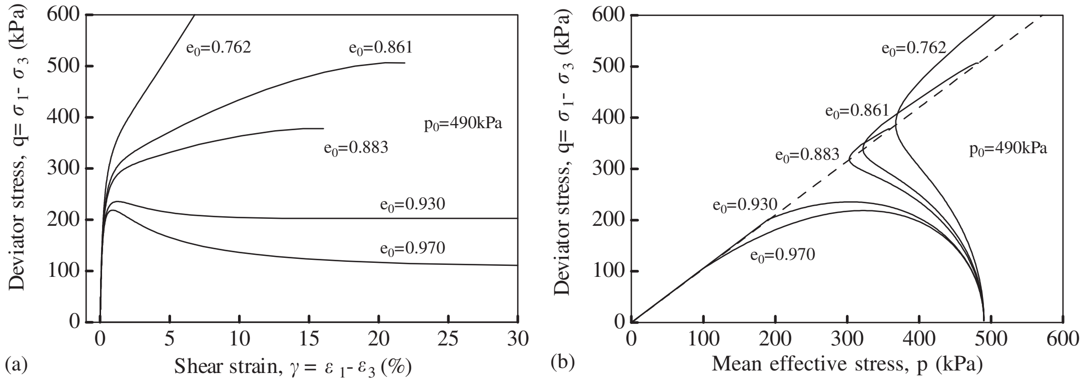

Figure 10. Effect of initial density on stress–strain behaviour of sand in undrained triaxial tests.

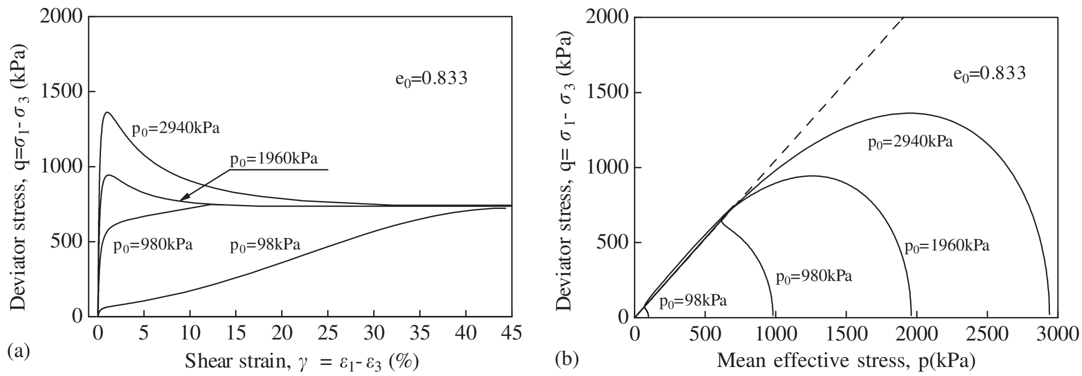

Figure 11. Effect of consolidation stress on stress–strain behaviour of sand in undrained triaxial tests.

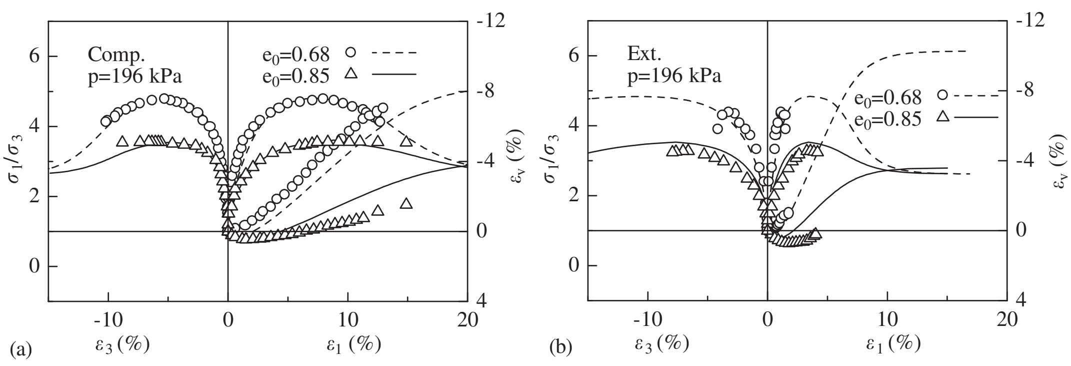

Figure 12. Comparison between predicted and observed stress–strain curves of Toyoura sand for $p =$ 196 kPa in drained triaxial tests (experimental data after Nakai *et al*. [13]).

model can predict the strength and dilatancy of sand for different initial void ratios not only in triaxial compression but also in triaxial extension.

5. CONCLUSIONS

A unified elastoplastic model was proposed, which can describe well the mechanical behaviour of sands at different values of void ratio and mean effective stress by introducing two state parameters χ_1 and χ_2. Parameter χ_1 is proposed to account for the deformation behaviour of the sands looser than RCL, while parameter χ_2 is proposed to describe the negative/positive dilatancy and the hardening/softening behaviour of the sands denser than RCL. The stress–strain behaviour of sands under three-dimensional stress conditions was modelled using a transformed stress tensor $\tilde{\sigma}_{ij}$ based on the SMP criterion.

ACKNOWLEDGEMENT

The writers thank Professor H. Matsuoka of Nagoya Institute of Technology for his invaluable help. The writers are also grateful to the reviewers for their constructive comments and useful suggestions for improvements on the paper. This study was supported by the National Natural Science Foundation of China, NSFC (No.10272010).

REFERENCES

1. Roscoe KH, Burland JB. On the generalised stress–strain behaviour of 'wet' clay. In *Engineering Plasticity*. Heyman J, Leckie FA (eds). Cambridge University Press: Cambridge, 1968; 535–609.
2. Yao YP, Matsuoka H, Sun DA. A unified elastoplastic model for clay and sand with the SMP criterion. *Proceedings of the 8th Australia New Zealand Conference on Geomechanics*, vol. 2, Hobart, 1999; 997–1003.
3. Matsuoka H, Yao YP, Sun DA. The Cam-clay models revised by the SMP criterion. *Soils and Foundations* 1999; **39**(1): 81–95.
4. Matsuoka H, Nakai T. Stress-deformation and strength characteristics of soil under three difference principal stresses. *Proceedings of the Japan Society of Civil Engineers* 1974; **232**:59–70.
5. Matsuoka H. On the significance of the spatial mobilized plane. *Soils and Foundations* 1976; **16**(1):91–100.
6. Verdugo R, Ishihara K. The steady state of sandy soils. *Soils and Foundations* 1996; **36**(3):81–91.
7. Luong MP. Stress–strain aspects of cohesionless soils under cyclic and transient loading. *International Symposium on Soils under Cyclic and Transient Loading* 1982; 315–324.
8. Ishihara K. Liquefaction and flow failure during earthquakes. The 33rd Rankine Lecture. *Geotechnique* 1993; **43**(3):351–415.
9. Bolton MD. The strength and dilatancy of sands. *Geotechnique* 1986; **36**(1):65–78.
10. Been K, Jefferies MG. A state parameter for sands. *Geotechnique* 1985; **35**(1):99–112.
11. Lee KL, Seed HB. Drained strength characteristics of sands. *Journal of Soil Mechanics and Foundation Engineering* (ASCE) 1967; **93**:117–141.
12. Sheng Y, Randolph MF. Effect of density state on the strength and deformation of sands. *Proceedings of the Pre-failure Deformation of Geomechanics*, vol. 1, Sapporo, 1994; 401–406.
13. Nakai T, Hoshikawa T, Hinokio M. Drained and undrained behaviour of sand in general stress systems. *Proceedings of the Deformation and Progressive Failure in Geomechanics*, Nagoya, 1997; 377–382.
14. Been K, Jefferies MG, Hachey J. The critical state of sands. *Geotechnique* 1991; **41**(3):365–381.
15. Jefferies MG. Nor-sand: a simple critical state model for sands. *Geotechnique* 1993; **43**(1):91–103.
16. Miura N, Murata H, Yasufuku N. Stress–strain characteristics of sand in a particle-crushing region. *Soils and Foundations* 1984; **24**(1):77–89.
17. Cubrinovski M, Ishihara K. Modelling of sand behaviour based on state concept. *Soils and Foundations* 1998; **38**(3):115–127.
18. Yoshimine M, Ishihara K. Flow potential of sand during liquefaction. *Soils and Foundations* 1998; **38**(3):189–198.

